CHEMIJA. 2008. Vol. 19. No. 1. P. 7–13

Effect of pulse plating on the composition and corrosion properties of Zn–Co and Zn–Fe alloy coatings

Rimantas Ramanauskas*,

Laima Gudavičiūtė,

Remigijus Juškėnas

Department of Metal Electrochemistry, Institute of Chemistry, A. Goštauto 9, LT-01108 Vilnius, Lithuania

Olga Ščit

Department of Chemistry, Vilnius Pedagogical University, Studentų 39, LT-08106 Vilnius, Lithuania

The influence of pulse plating parameters on the chemical and phase composition, surface topography and corrosion resistance of Zn–Co (<1%) and Zn–Fe (<1%) alloy coatings has been studied. Pulse plating of low-alloyed Zn coatings resulted in the grain size reduction of deposits, however, this process was not accompanied by any significant reduction in the corrosion currents of these alloys. It was suggested that the dual phase formation was the principal reason why pulse plated low-alloyed Zn coatings did not exhibit any improvement in their corrosion resistance.

Key words: pulse electrodeposition, zinc alloys, phase composition, corrosion

INTRODUCTION

The service life of sacrificial zinc electrodeposits can be increased by means of alloying with relatively more noble Fe group metals. The most common alloys exhibiting good protective properties contain 10–15% Ni [1–10], while less than 1% is needed when Co or Fe are added to the Zn matrix to achieve the optimum functional properties [6, 11–18]. Alloy coatings appeared to be attractive, since under similar electroplating conditions these deposits in addition to lower corrosion rates possess better physical properties than those of pure Zn layer. For example, such coatings are able to withstand exposure to high temperatures (~300 °C), maintaining similar corrosion properties and good adhesion to a substrate [3], which improves the ability of paint to adhere to the surface of steel [14, 16].

However, the permanent requirement of the industry (especially the automobile industry) to reduce the thickness of the coatings and to increase corrosion resistance encourages the development of new surface finishing processes for zinc plating.

Pulse electrodeposition can be used as a means for producing unique structures, i. e. coatings with properties unachievable by direct current (d. c.) plating. The application of non-stationary electrodeposition yields smoother and denser deposits with negligible porosity, therefore, pulse plating is one of the methods to obtain coatings that are more resistant to corrosion. However, non-equilibrium crystallization may result in the changes of the alloy phase composition, which may also affect the corrosion performance of the coating.

Acidic or alkaline plating baths can be used for the plating of Zn and Zn alloys. The published data on pulse-plated Zn alloys are mostly related to coatings deposited from acidic solutions [6, 19–24]. For example, it is known, that d. c. electrodeposition of a Zn–Ni alloy in an acidic bath results in the formation of a dual phase structure [25], which causes a significant reduction in the corrosion resistance of the coating. Meanwhile, deposition in alkaline solutions, in contrast to the acidic ones, is less efficient, but gives a more uniform plating and results in the formation of a single-phase Zn–Ni alloy [25, 27]. In addition, pulse plating effect on the phase composition of low-alloyed Zn coatings with Fe and Co has not been investigated to date.

The objective of the present investigation was to determine the influence of pulse electrodeposition parameters on the phase composition and corrosion properties of Zn–Co (<1% Co) and Zn–Fe (<1% Fe) alloy coatings.

EXPERIMENTAL

Zn–Co and Zn–Fe coatings of ~9 μm thickness were electrodeposited on low carbon steel (C 0.05–0.12%, Mn 0.25–0.5%) samples, which were polished mechanically to a bright mirror. An alkaline cyanide-free plating solution contained ZnO 10 g l^{-1}, NaOH 100 g l^{-1} and organic additives. A detailed description of the plating bath and operating conditions are presented elsewhere [26–29].

* Corresponding author. E-mail: ramanr@ktl.mii.lt

The Zn alloy coatings were deposited at 25 °C varying the cathodic peak current density (i_p) from 0.05 to 1 A cm^{-2}, current on-time (t_{on}) – from 0.1 to 2 ms and current off-time (t_{off}) – from 1 to 10 ms. The electrodeposition experiments were carried out by varying one parameter at a time with other parameters being fixed at standard conditions. The Zn–Fe coatings were deposited under the following fixed plating parameters: i_p = 0.1 A cm^{-2}, t_{on} = 0.2 ms, t_{off} = 2 ms and Zn–Co: i_p = 0.2 A cm^{-2}, t_{on} = 0.2 ms, t_{off} = 2 ms. Current efficiency of the plating process varied between 40% and 80%.

The d. c. plated Zn–Fe and Zn–Co coatings were obtained under 0.025 A cm^{-2} current density.

X-ray diffraction measurements were performed with a D8 diffractometer equipped with a Göbel mirror (primary beam monochromator) for Cu radiation. A step-scan mode was used in the 2-theta range from 30° to 75° with a step length of 0.02° and a counting time of 5 s per step.

The chemical composition of the electrodeposited coatings was determined applying electron probe microanalysis with SEM JXA-50A.

Surface morphology studies were carried out with an AFM by an Explorer (VEECO-Thermomicroscopes) scanning probe microscope at atmospheric pressure and room temperature in a contact mode. A Si_3N_4 cantilever with the force constant of 0.032 N m^{-1} was used and the obtained resolution of the images was 300 × 300 pixels. The grain size dimensions of the electrodeposited coatings were determined by means of SPMLab software and from profile line analysis.

The corrosion behaviour of the coatings was investigated in an aerated stagnant 0.6 M NaCl + 0.2 M $NaHCO_3$ solution (pH 6.8) using a standard three-electrode system with a Pt counter electrode, a saturated calomel reference electrode and a PI-50 potentiostat. The corrosion current densities (i_{corr}) were determined from Tafel plot extrapolation. To begin the measurements, the sample was introduced into the cell immediately after electroplating and was allowed to equilibrate, which usually took 15 min. Polarization measurements were performed under potentiodynamic conditions with a potential scan rate of 0.1 mV s^{-1}.

RESULTS AND DISCUSSION

Chemical composition

The principal requirements for the pulse plated Zn alloys were the absence of macrostructural defects, such as dendrites or areas of local dissolution on the surface of the coating, and the stability of the alloy composition. The latter implied a variation in Co and Fe concentrations in the alloy between 0.4–1.0%. The concentrations of alloying metals in the deposit lower than 0.4% do not exhibit any beneficial effect on the corrosion properties of coatings with respect to that of pure Zn, while a higher amount of Co and Fe in the alloy results in the dual phase formation [1, 29].

The data on the composition, structure and corrosion behaviour of Zn–Co and Zn–Fe coatings deposited in an alkaline bath by a direct current have been presented in our previous studies [26–30]. It was established there that the low-alloyed deposits were single-phase solid solutions of Co and Fe in Zn with 0.6% and 0.5% concentration of the alloying metals, respectively.

The influence of pulse plating parameters: cathodic peak current density (i_p), current on-time (t_{on}) and current off-time (t_{off}) on the amount of the alloying elements is presented in Fig. 1. Electrodeposition conditions affected the composition of Zn alloys in the following manner: the increase in i_p and t_{off} caused an increase in the amount of both alloying metals in the deposit, while the variation in t_{on} affected the composition of each alloy in a different mode – an increase in Co amount was observed with the increase in t_{on} values, whereas the variation of this parameter had no significant influence on the amount of the deposited Fe in the alloy, as its concentration changed in a narrow range between 0.8 and 0.9%. Meanwhile, i_p and t_{off} variations caused an increase in the Fe amount up to 1.2 and 1.5%, when i_p and t_{off} higher than 0.7 A cm^{-2} and 2 ms were applied, respectively, (Fig. 1 a, c). The latter cases were not acceptable, as the limiting concentration of the alloying element (1%) was overpassed. Besides, the quality of the deposits, when t_{off} higher than of 5 ms was applied, was insufficient. An increase in i_p, t_{on} and t_{off} caused an increase in the Co amount in the deposit, however, the concentration of this metal varied in the range between 0.5 and 0.8%. The presented dependences (Fig. 1) validate the optimal range of pulse plating parameters, which ensured the desirable composition of Zn alloys.

Topography

Surface topography studies were based on AFM measurements with the aim to determine the influence of plating parameters on the grain size dimensions, as well as to find out the deposition conditions, which resulted in the surface macro-structural defect formation. The images representing the influence of pulse plating parameters on the surface structure of Zn–Co and Zn–Fe coatings are presented in Figs. 2–4.

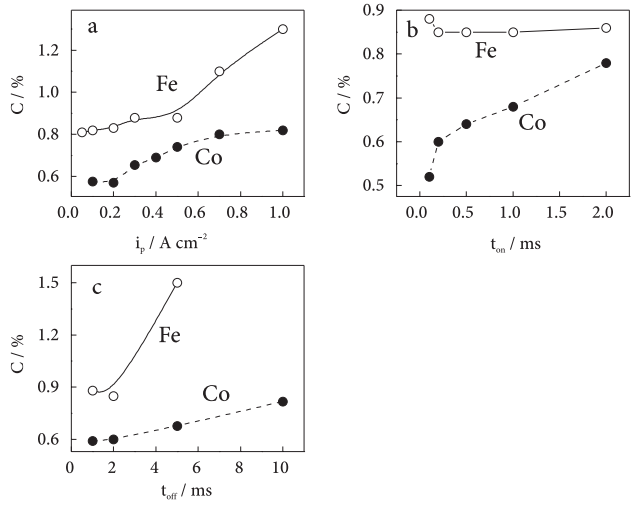

Fig. 1. Effect of pulse plating parameters on the amount of alloying metals in the deposits

The investigations on μm level (20 × 20 μm scanned surface area) have shown that the morphology of both alloy coatings was very similar; therefore, only the images of Zn–Co of the mentioned scanned area are presented. D. c. plated Zn–Co and Zn–Fe coatings consisted of micron and sub-micron sized granular crystallite agglomerations (Fig. 2 a). The size of these formations (Δ_{ag}) varied

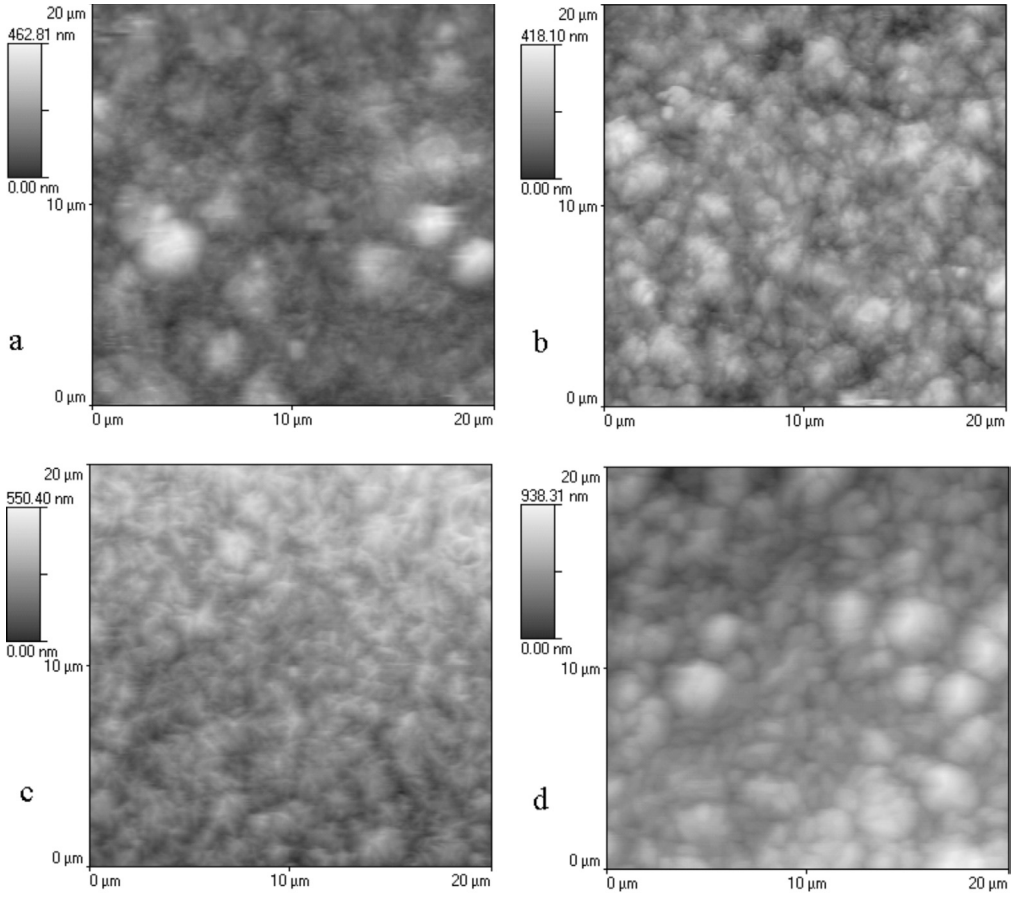

Fig. 2. AFM images of Zn–Co coatings deposited under: *a* – d. c. conditions; *b, c, d* – pulse-plated under cathodic peak current density i_p (A cm^{-2}): *b* – 0.2, *c* – 0.3, *d* – 1. The scanned area is 400 µm^2

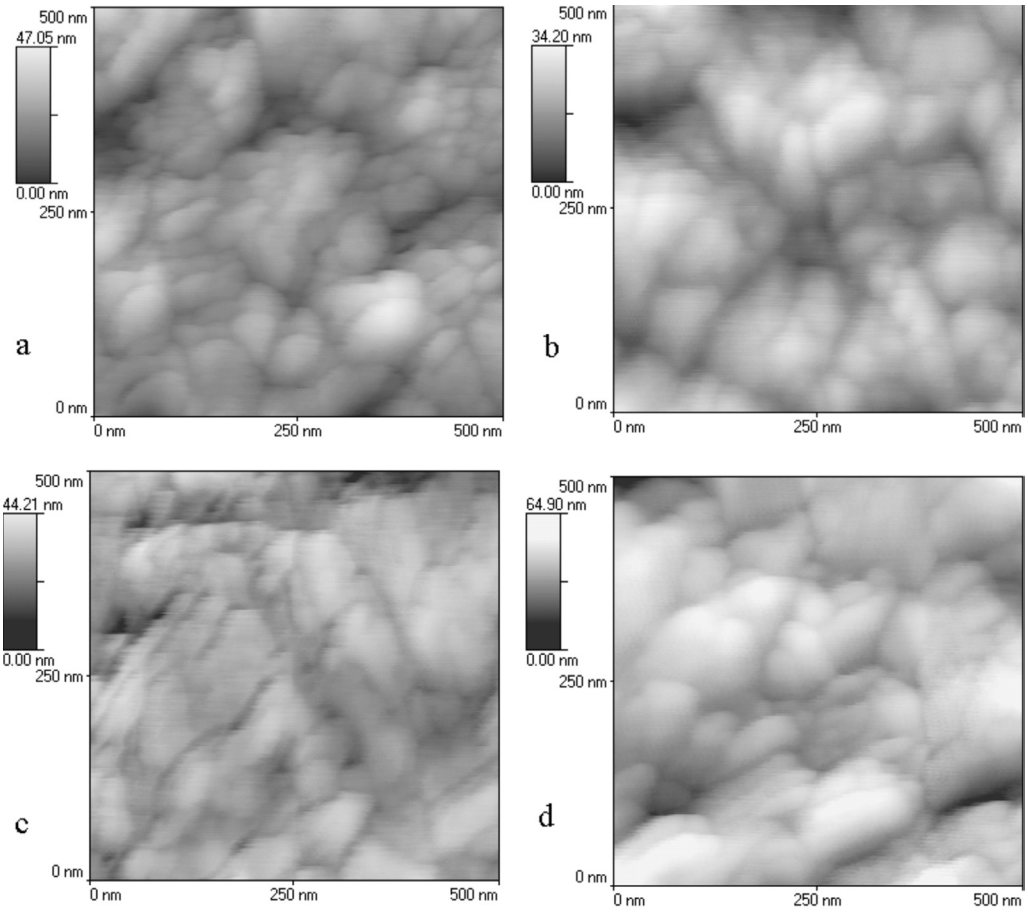

Fig. 3. AFM images of Zn–Co coatings deposited under: *a* – d. c. conditions; *b, c, d* – pulse-plated under cathodic peak current density i_p (A cm^{-2}): *b* – 0.2, *c* – 0.3, *d* – 1. The scanned area is 0.25 µm^2

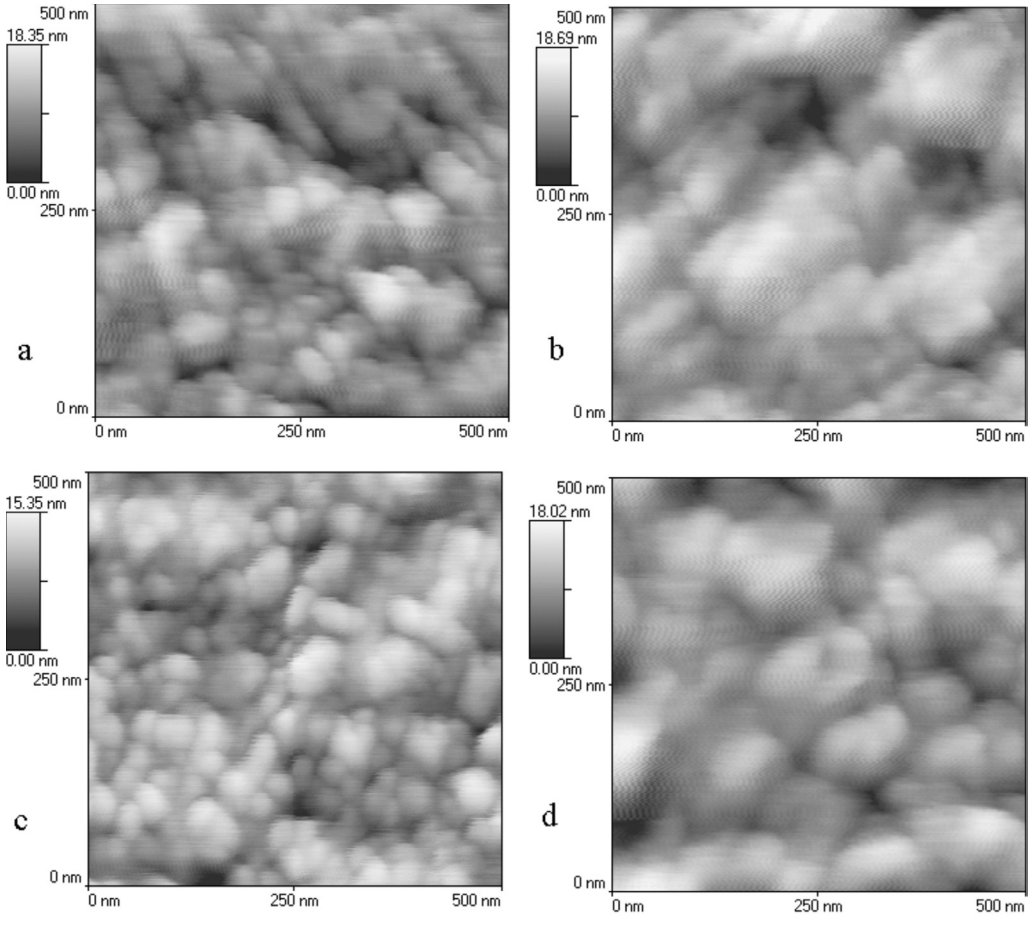

Fig. 4. AFM images of Zn–Fe coatings deposited under: *a* – d. c. conditions; *b, c, d* – pulse-plated under cathodic peak current density i_p (A cm^{-2}): *b* – 0.1, *c* – 0.2, *d* – 1. The scanned area is 0.25 μm^2

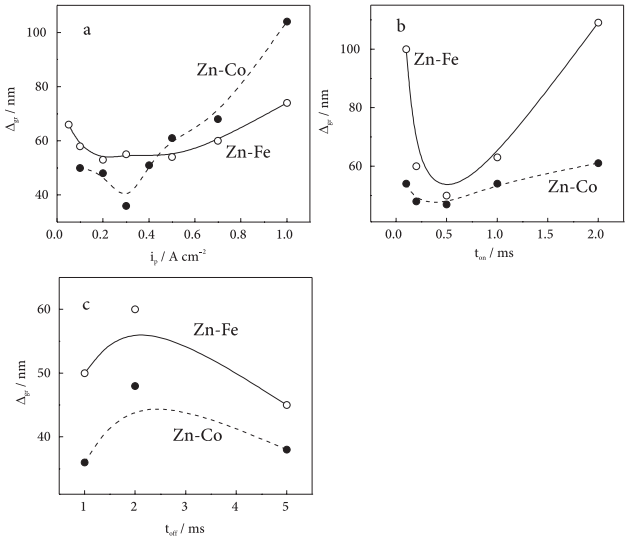

Fig. 5. Effect of pulse plating parameters on the grain size dimensions (Δ_{gr}) of pulse plated Zn–Co and Zn–Fe coatings

in the range from 0.4 to 2.5 μm with the average values of 0.9 and 1.31 μm for Zn–Co and Zn–Fe, respectively.

The ultrafine-grained structure was determined from a scanned area of 500 × 500 nm, and it appeared that the average grain size (Δ_{gr}) values for d. c. plated samples were 61 nm and 72 nm for Zn–Co (Fig. 3 a) and Zn–Fe (Fig. 4 a) coatings, respectively. The grain size dimensions of the deposited coatings have been determined on the basis of AFM measurements and are presented in Fig. 5. It has been shown in our previous study with pulse-plated Zn coatings [36] that the grain size values obtained by this technique coincide well with the results of XRD measurements. A comparison of crystallite agglomeration and grain size dimensions with the data on corrosion behaviour of pulse-plated Zn coatings implied that corrosion resistance was related more to Δ_{gr} values than to Δ_{ag} ones [36]. Therefore, the main attention in this study was paid to Δ_{gr} values of the plated Zn–Co (Fig. 3) and Zn–Fe (Fig. 4) coatings.

All the pulse-plated samples were obtained with higher cathodic current densities than the d. c. deposits. It is well known that low overpotential deposition produces films with large surface irregularities, whereas high overpotential deposition yields films with smooth surfaces [31, 32]. A raise in the overpotential increases the free energy to form new nuclei, which results in a higher nucleation rate and a smaller grain size. The influence of i_p on the surface morphology of pulse plated Zn–Co and Zn–Fe coatings can be observed from AFM images presented in Figs. 3 and 4, respectively.

The main difference in the topography of Zn–Co and Zn–Fe electrodeposits obtained by d. c. and pulse techniques was in the size of crystallite agglomerations (Fig. 2) and grains (Figs. 3 and 4). Pulse-plated coatings were more compact and possessed more homogeneous structures with the minimal values of Δ_{ag} 0.67 and 0.69 μm for Zn–Co and Zn–Fe, respectively (Fig. 2). The increase in the cathodic current of pulse plating from 0.1 to 0.3 A cm^{-2} led to the reduction of the average Δ_{gr} from 50 to 36 nm and from 68 to 55 nm for Zn–Co and Zn–Fe, respectively.

However, a further increase in i_p (>0.3 A cm^{-2} and >0.5 A cm^{-2} for Zn–Co and Zn–Fe, respectively) resulted in the origination of discrete large crystallites, possibly the germs of dendrites (Fig. 2 d), which caused both a reduction of the homogeneity of grain distribution and an increase in the grain size of both alloy coatings (Fig. 5 a).

The nucleation rate is enhanced and the grain size of the deposit usually decreases because of higher i_p; however, the effect of t_{on} and t_{off} on the deposit characteristics for a certain system cannot be predicted, because the crystallization is strongly influenced by the composition of the plating bath and, hence adsorption / desorption phenomena. Therefore, during the electrocrystallization, each system may react differently yielding a different surface morphology. The variation in t_{on} and t_{off} parameters did not cause an occurrence of any new morphological features of Zn–Co and Zn–Fe deposits on the nano-metric scale, therefore, the corresponding images are not given, while the curves depicting the influence of these parameters on the values of Δ_{gr} are presented in Fig. 5.

The variation in t_{on} from 0.1 to 0.5 ms caused a slight decrease in Δ_{gr} values of Zn–Co coating from 58 to 43 nm with a further increase in Δ_{gr} values up to 60 nm at t_{on} 2 ms. Meanwhile, the effect of this parameter on the grain size of Zn–Fe deposits was more significant (Fig. 5 b). The lowest t_{on} values applied (0.1 ms) resulted in deposition of a Zn–Fe coating with the grain size close to 100 nm, which is higher than that of the d. c. plated sample. The minimal Δ_{gr} values (~54 nm) were obtained at t_{on} 0.5 ms, with a further sharp increase in Δ_{gr} at higher t_{on}, which was even higher than 100 nm at t_{on} 2 ms. The reoccurrence of large crystallites at the longest t_{on} was the reason of a significant increase in Δ_{gr}.

In pulse plating, there is no applied current during the t_{off} period, and whether fine-grained deposits are obtained in practice or not depends upon what happens during this period. Zn alloy pulse deposition was carried out in the t_{off} range from 1 to 10 ms, however, because of insufficient quality of the coatings deposited at t_{off} >5 ms, a precise determination of Δ_{gr} values was inexpedient. The Δ_{gr} values of both deposited alloys increase when t_{off} increases from 1 to 2 ms (from 35 nm to 48 nm and from 50 nm to 60 nm for Zn–Co and Zn–Fe, respectively) with a further gradual decrease, when t_{off} changes from 2 to 10 ms up to the initial Δ_{gr} values (Fig. 5 c). If t_{off} is long enough, the areas of local dissolution can be produced on the deposited metal surface [25, 33]. Such an effect was observed for pure Zn coatings [36] at t_{off} higher than 20 ms. In the case of pulse-plated low-alloyed Zn deposits, an application of even t_{off} >5 ms caused an undesirable increase in the Fe amount in the alloy (Fig. 1) and led to poor quality of Zn–Co coating (powder-like).

The occurrence of the macrostructural defects on the surface of pulse-plated Zn alloys and the insufficient quality of the coatings limited the application of higher values of the parameters i_p, t_{on} and t_{off}. Generally, the grain size of Zn–Co coatings obtained under the pulse plating conditions appeared to be slightly lower with respect to that of Zn–Fe deposits.

Corrosion behaviour

Corrosion behaviour of the pulse-plated Zn coatings was investigated in a naturally aerated NaCl + $NaHCO_3$ solution at pH 6.8. It is known, however, that corrosion rates measured electrochemically are inconsistent with the atmospheric data mainly because of the presence of corrosion products on the surface. Zn corrosion in an unbuffered Cl^- solution occurs with the formation of a porous oxide film [34]. However, in a HCO_3^- containing media, the oxide film is supposed to be more compact, adherent and less soluble, thus, exhibiting a passivating character [35]. Aqueous corrosion data for Zn alloy samples in a HCO_3^- containing media correlate well with the atmospheric corrosion data [30]. Therefore, this solution was applied.

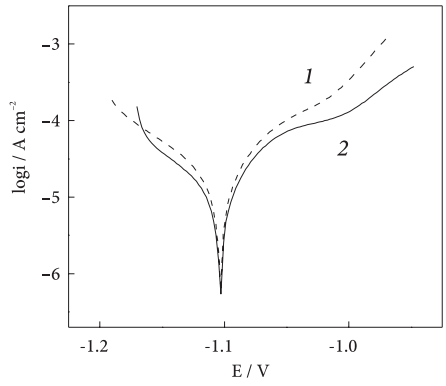

Fig. 6. Polarization curves of pulse-plated Zn alloy electrodes in 0.6 M NaCl + 0.2 M $NaHCO_3$ solution: *1* – Zn-Co, *2* – Zn–Fe. Potential sweep rate is 0.1 mV s^{-1}

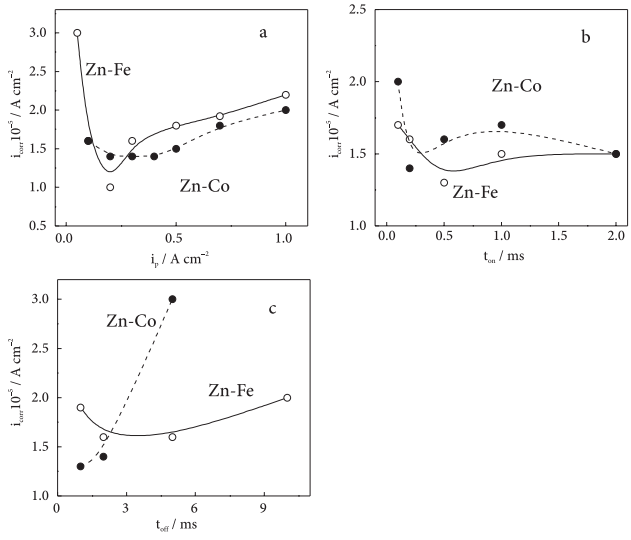

Fig. 7. Effect of the pulse plating parameters on the corrosion current (i_{corr}) of Zn–Co and Zn–Fe alloy coatings in 0.6 M NaCl + 0.2 M $NaHCO_3$ solution

The polarization curves of Zn alloys in a test media are presented in Fig. 6. No significant differences were found in the shape of polarization curves for various investigated coatings, thus there are only the polarization curves for each alloy sample presented. The corrosion current densities (i_{corr}) were determined from Tafel plot extrapolation. They were obtained from a computer data fit, and the obtained results are presented in Fig. 7.

The i_{corr} values of pulse-plated Zn alloy coatings varied in the range from $1.0 \cdot 10^{-5}$ to $3.0 \cdot 10^{-5}$ A cm^{-2}. The minimal values of i_{corr} ($1.0 \cdot 10^{-5}$ A cm^{-2}) for pulse plated Zn–Fe alloy were obtained at a single value of ip – 0.2 A cm^{-2}, with a further increase in i_{corr} up to $2.0 \cdot 10^{-5}$ A cm^{-2} when i_p values higher than 0.5 A cm^{-2} were applied (Fig. 7 a). Meanwhile, i_{corr} values of Zn–Co alloy with the variation of i_p varied in a very narrow range (close to $1.5 \cdot 10^{-5}$ A cm^{-2}).

Generally, the influence of t_{on} on the variation of i_{corr} values of the deposited coatings was not significant, as i_{corr} varied between $1.9 \cdot 10^{-5}$ and $1.3 \cdot 10^{-5}$ A cm^{-2}. A slight reduction in i_{corr} values was observed for both investigated Zn alloy coatings with the increase in t_{on} only in the initial range from 0.1 to 0.2 ms for Zn–Co and from 0.1 to 0.5 for Zn–Fe.

Pulse deposition of Zn alloys was carried out with t_{off} values varying in the range from 1 to 10 ms. Generally, the increase in t_{off} of the Zn alloy deposition was not an effective means for the improvement of corrosion behaviour of the coatings obtained. The increase in this parameter from 1 to 5 or 10 ms caused a nearly threefold increase in i_{corr} values of the pulse plated Zn–Co alloys, meanwhile, it did not significantly effect i_{corr} values of Zn–Fe coatings (Fig. 7 c), which varied between $1.7 \cdot 10^{-5}$ and $1.9 \cdot 10^{-5}$ A cm^{-2}.

Summarizing the results on corrosion behaviour of the pulse-plated Zn alloys, it can be stated that Zn–Co and Zn–Fe coatings, except the t_{off} variation, exhibited a similar corrosion behaviour, while in general, the application of pulse plating was not of great significance for the corrosion resistance enhancement of these alloys, as the i_{corr} values of d. c. plated alloys were $1.5 \cdot 10^{-5}$ A cm^{-2} and $1.9 \cdot 10^{-5}$ A cm^{-2} for Zn–Co and Zn–Fe, respectively, while pulse electrodeposition of Zn coatings resulted in nearly fourfold reduction in the corrosion currents in comparison with the direct current plated samples [36].

Phase composition

The influence of pulse plating parameters on the phase composition of the deposited alloys can be determined from XRD data. Figure 8 a depicts the XRD patterns for the pulse-plated zinc alloy coatings.

Pure Zn and low-alloyed coatings with Co and Fe electrocrystallize with a distorted form of hexagonal close packing. The pulse plated Zn–Co and Zn–Fe coatings exhibited sharp peaks corresponding to Zn and Fe (base metal). However, two different phases of Zn can be identified for all the deposited low-alloyed Zn coatings. The first one is an α-phase or the solid solution of Co or Fe in Zn. This statement is reasoned in Figure 8 b, where some fragments of XRD patterns for Zn–Co and Zn–Fe coatings are presented. The maxima of XRD peaks Zn 10.0 and Zn 10.1 (dashed vertical lines) are shifted with respect to the position of these peaks for the pure Zn (solid vertical lines) (PDF 04-0831), while the peak Zn 00.2 nearly coincides with that for the latter. However, one more peak can be seen in the vicinity of this peak at higher diffraction angles. The peaks 10.0 and 10.1 are obviously attributed to the α-phase. The lattice parameters *a* and *c* of the α-phase can be calculated using Θ angle of the maximum of the peaks 10.0 and 10.1, respectively. Having determined the lattice parameter *c*, one can calculate 2 Θ angle of the maxima of the peaks Zn–Co 00.2 and Zn–Fe 00.2, which are represented by dashed vertical lines in Figure 8 b. These lines coincide with the peaks, which are in the vicinity of that for pure Zn 00.2. So, these low intensity peaks on XRD patterns for Zn–Co and Zn–Fe are attributable to the α-phase. Consequently, the pulse plated coatings of Zn–Co and Zn–Fe are mixtures of two phases, one of them being the α-phase and the other – pure zinc or the α-phase with a significantly lower proportion of Co or Fe.

Although during previous corrosion behaviour studies of d. c. plated Zn alloy coatings it was established that Zn–Co exhibited from two- to three-fold lower atmospheric corrosion rates than pure Zn [26, 30], the results of the electrochemical measurements

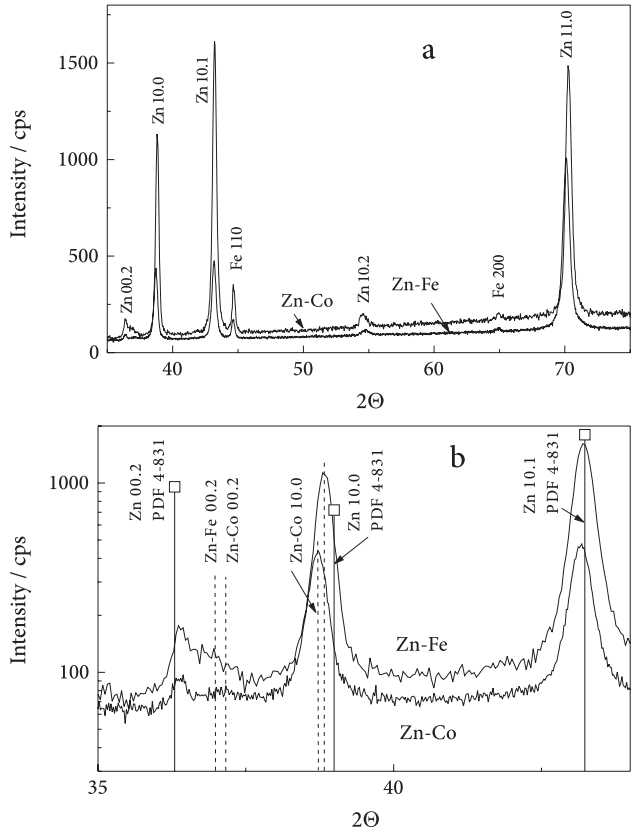

Fig. 8. XRD patterns of pulse-plated Zn–Co and Zn–Fe coatings under cathodic peak current density i_p 0.5 A cm^{-2}

indicated that both these alloys possessed almost twice as low corrosion currents compared to those of Zn coatings [26], and corrosion performance of Zn–Fe deposits was similar to that of Zn under both conditions. Pulse electrodeposition of Zn coatings appeared to be beneficial in the grain size and corrosion rate reduction, (e. g., a fourfold reduction in the corrosion current in comparison with d. c. plated samples was observed) [36], while the pulse-plated low-alloyed Zn coatings did not exhibit any significant improvement in their corrosion resistance.

CONCLUSIONS

Pulse electroplating of Zn alloys in comparison with direct current deposition resulted in the grain size reduction from 61 nm to 36 nm and from 72 nm to 50 nm for Zn–Co and Zn–Fe coatings, respectively. However, the correspondent reduction in the corrosion currents of these alloys was not observed.

Non-stationary crystallization produced two different phases of Zn during Zn–Co and Zn–Fe plating. The low-alloyed coatings obtained by pulse deposition presented a mixture of two phases; one of them was the α-phase and the other was pure Zn or the α-phase with a significantly lower concentration of Co or Fe. It could be supposed that one of the principal reasons, why the pulse-plated Zn–Co and Zn–Fe coatings did not exhibit a reduction in their corrosion currents was the formation of a dual phase during the pulse deposition.

Received 11 December 2007
Accepted 19 December 2007

References

1. D. E. Hall, *Plating and Surf. Finish*., **70**, 59 (1983).
2. L. Felloni, R. Fratesi, E. Quadrini, G. Roventi, *J. Appl. Electrochem*., **17**, 574 (1987).
3. N. Zaki, *Metal Finish.*, **87**, 57 (1989).
4. D. A. Wright, N. Gage, *Trans. IMF*, **72**, 130 (1994).
5. N. R. Short, A. Abibsi, J. K. Dennis, *Trans. IMF*, **67**, 73 (1989).
6. G. D. Wilcox, D. R. Gabe, *Corros. Sci*., **35**, 1251 (1993).
7. K. R. Baldwin, C. J. E. Smith, *Corrosion*, **51**, 932 (1995).
8. K. R. Baldwin, C. J. E. Smith, *Trans. IMF*, **74**, 202 (1996).
9. A. M. Alfantazi, U. Erb, *Corrosion*, **52**, 880 (1996).
10. L. Fedrizzi, R. Fratesi, G. Lunazzi, G. Roventi, *Surf. Coat. Technol*., **53**, 171 (1992).
11. A. P. Shears, *Trans. IMF*, **67**, 67 (1989).
12. A. Stankevičiūtė, L. Leinartas, G. Bikulčius, D. Virbalytė, A. Sudavičius, E. Juzeliūnas, *J. Appl. Electrochem.,* **28**, 89 (1998).
13. R. Fratesi, G. Roventi, C. Branca, S. Simoncini, *Surf. Coat. Technol*., **63**, 97 (1994).
14. J. Ch. Chang, H. Wei, *Corros. Sci*., **30**, 831 (1990).
15. G. Beck Nielsen, M. Kjaer Larsen, K. A. Jensen, D. Ulrich, *Corros. Sci*., **30**, 1907 (1990).
16. J. Giridhar, W. J. Ooij, *Surf. Coat. Technol*., **53**, 35 (1992).
17. Z. Zhang, W. H. Leng, H. B. Shao, J. Q. Zhang, J. M. Wang, C. N. Cao, *J. Electroanal. Chem*., **516**, 127 (2001).
18. J. L. Ortiz-Aparicio, Y. Meas, G. Trejo, R. Ortega, T. W. Chapman, E. Chainet, P. Ozil, *Electrochim. Acta*, **52**, 4742 (2007).
19. K. Kondo, M. Yokoyama, K. Shinohara, *J. Electrochem. Soc*., **142**, 2256 (1995).
20. F. Y. Ge, S. K. Xu, S. B. Yao, S. M. Zhou, *Surf. Coat. Technol*., **88**, 1 (1996).
21. Y. Tsuru, H. Egawa, *Denki Kagaku*, **64**, 112 (1996).
22. Y. Tsuru, H. Egawa, *Denki Kagaku*, **65**, 143 (1997).
23. H. Ashassi-Sorkhabi, A. Hagrah, N. Parvini-Ahmadi, J. Manzoori, *Surf. Coat. Technol*., **140**, 278 (2001).
24. J-Y. Fei, G. D. Wilcox, *Electrochim. Acta,* **50**, 2693 (2005).
25. N. V. Mandich, *Metal Finishing*, **98**, 375 (2000).
26. R. Ramanauskas, *Appl. Surf. Sci*., **153**, 53 (1999).
27. R. Ramanauskas, R. Juškėnas, A. Kaliničenko, L. F. Garfias-Mesias, *J. Solid State Electrochem*., **8**, 416 (2004).
28. M. A. Pech-Canul, R. Ramanauskas, L. Maldonado, *Electrochim. Acta,* **42**, 255 (1997).
29. R. Ramanauskas, L. Gudavičiūtė, L. Diaz-Ballote, P. Bartolo-Perez, P. Quintana, *Surf. Coat. Technol*, **140**, 109 (2001).
30. R. Ramanauskas, L. Muleshkova, L. Maldonado, P. Dobrovolskis, *Corros. Sci*., **40**, 401 (1998).
31. R. T. C. Choo, J. M. Toguri, A. M. El-Sherik, U. Erb, *J. Appl. Electrochem*., **25** 348 (1995).
32. N. Ibl, J. Cl. Puipe, H. Angerer, *Surf. Technol*., **6**, 287 (1978).
33. R. Ramanauskas, L. Gudavičiūtė, A. Kaliničenko, R. Juškėnas, *J. Solid State Electrochem*., **9**, 900 (2005).
34. T. E. Graedel, *J. Electrochem. Soc*., **136**, 193C (1989).
35. R. Guo, F. Weinberg, D. Tromans, *Corrosion*, **51**, 356 (1995).
36. R. Ramanauskas, L. Gudavičiūtė, R. Juškėnas, O. Ščit, *Electrochim. Acta*, **53**, 1801 (2007).

Rimantas Ramanauskas, Laima Gudavičiūtė, Remigijus Juškėnas, Olga Ščit

IMPULSINĖS ELEKTROLIZĖS ĮTAKA Zn–Co IR Zn–Fe ELEKTROLITINIŲ LYDINIŲ SUDĖČIAI IR KOROZINĖMS SAVYBĖMS

S a n t r a u k a

Darbe buvo tiriama impulsinės elektrolizės parametrų įtaka Zn–Co ir Zn–Fe elektrolitinių lydinių cheminei ir fazinei sudėčiai, paviršiaus topografijai ir dangų korozinėms savybėms. Impulsinės elektrolizės taikymas mažai legiruotiems Zn lydiniams nusodinti įgalino sumažinti dangų kristalitų dydžius, tačiau jų korozinio atsparumo pagerėjimo nepasiekta. Padaryta prielaida, kad dangų korozijos greičio sumažinti nepavyksta dėl dvifazio lydinio susidarymo impulsinės elektrolizės metu. Rentgeno difrakciniais tyrimais nustatyta, kad mažai legiruoti Zn lydiniai sudaryti iš α-fazės (kieto Co ar Fe tirpalo Zn) ir gryno Zn fazės.